Response Surface Methodology for Optimization of Solar Photo-Oxidation of Direct Violet 51 on TiO_2 and ZnO

Boutra, Belgassim*[*+]*; Sebti, Aicha

Unité de Développement des Equipements Solaires, UDES/Centre de Développement des Energies Renouvelables, CDER, Bou Ismail, Tipaza, ALGERIA

Ouldamar, Abdelghani; Hachemi, Nadir

Saad Dahlab University– Faculty of Technology, Route de Soumaa, Blida, ALGERIA

Mohamed, Trari

Laboratory of Storage and Valorization of Renewable Energies, USTHB, Algiers, ALGERIA

ABSTRACT: *This work is a study of the optimization of the removal of a textile azo dye namely Direct Violet 51 (DV 51) by heterogeneous solar photocatalysis onto ZnO and TiO_2. The Response Surface Methodology (RSM) was applied to design the experiments and to investigate the interactions between the physical parameters including the type of catalyst. Based on the results, a degradation efficiency of 100 % was obtained for the ZnO/Solar light system in the optimal conditions (catalyst dose = 0.1567 g/L, C_O = 10 ppm, and reaction time = 120 min). Appropriate figures of merit were selected for evaluating the energy requirement for DV 51 removal. The estimation of collector area per order and electric energy per order confirmed that the ZnO photocatalytic system used the introduced light more efficiently both under artificial and solar light. According to the scavenging mechanism study, superoxide ($O^{\bullet}_2^-$) and electrons (e^-) are the main species responsible for DV 51 degradation by ZnO.*

KEYWORDS: *Direct Violet 51; D-optimal design; RSM; Solar photocatalysis; TiO_2; ZnO; Figures of merit.*

INTRODUCTION

Industrialization is a large contributor to water scarcity not only by depleting freshwater resources but also by releasing huge volumes of highly toxic wastewater [1–3]. Textile processing is one of the main consumers of water after the oil and paper industries. It's estimated that textile production requires around 79 trillion liters of water annually and this makes this sector responsible for over 20% of global industrial water pollution [4]. Textile wastewaters are characterized by a large Chemical Oxygen Demand (COD), pH, and temperature. They are strongly colored and show low biodegradability attributed to the existence of synthetic and natural dyes. Currently, the major challenge facing textile factories is the elimination of synthetic dyes from industrial effluents owing to their

* *To whom correspondence should be addressed.*
+ *E-mail: boutrabelkacem@gmail.com*
1021-9986/2024/3/1140-1155 16/$/6.06

toxicity as well as mutagenic and carcinogenic effects [1–4]. Moreover, because of their complex and mesomeric structure and synthetic origin, these dyes are persistent to biological mineralization. In order to meet the water quality requirements for discharges imposed by governments and move toward a circular economy for textiles, industries have to seek for more efficient and sustainable strategies for the wastewater treatment such as Advanced Oxidation Technologies (AOTs) [2,5–11]. Wastewater treatment using AOPs can lead to total mineralization of recalcitrant organic pollutants or formation of less or non-toxic intermediates [9,12–16]. AOPs achieve this conversion by generating strong oxidant agents, especially hydroxyl and oxygen radicals, which are non-selective as they are able to destroy most of the organic pollutants. The principal advantage of AOPs, is that the production of radicals can be performed by using different energy sources: electrical energy, chemical energy and radiant energy. The sustainability and economic viability of AOPs can be enhanced by using solar energy rather than commercial radiation sources [8,17–22]. Photocatalysis is a heterogeneous advanced oxidation technology, where light is used to initiate the hydroxyl radicals formation by activating the surface of a catalyst. ZnO and TiO_2 are widely employed because they exhibit excellent chemical/photochemical stability, good biocompatibility and nontoxicity [6, 34–37]. Despite the poor activation of these two catalysts under solar light, TiO_2 and ZnO being the materials of choice in most photocatalytic processes. The availability of solar energy in Algeria presents a key factor to promote sustainable and cost effective photocatlytic process. In this work, we aimed to assess the ability of solar energy to remove a textile dye, namely Direct Violet 51 (DV 51) from a synthetic solution using ZnO and TiO_2. This azo dye was selected because only a few works have been devoted to study its photocatalytic degradation. DV 51 was successfully removed from synthetic solution after photocatalysis using immobilized titanium dioxide reactor illuminated by artificial UV light [27]. The photocatalytic activity of synthetic catalyst (CeO_2/rGO-HYBD) have been assessed towards the degradation of DV 51 under both UV and solar radiations. The new catalyst allowed the removal of almost 93% of dye [28]. Other remediation alternatives have been used to eliminate DV 51 such as adsorption [16,29], biosorption [14], electrochemical, biological and biotechnological processes [15,30,31]. Among these methods, electrochemical and biotechnological processes have exhibited the highest removal performance. In the present study, solar photocatalytic degradation of DV 51 was performed using available and inexpensive catalysts. The optimal degradation parameters of the textile dye were identified using response surface methodology (RSM) because practical applications of photocatalysis require a range of conditions in which they can perform. In addition, this work explored new approach for prioritizing photocatalytic processes based on the evaluation of the energetic efficiency of photocatalytic processes. The figures of merit recommended by IUAPAC namely the electric energy and the solar collector area were employed to estimate the energy consumption for removing DV 51.

Optimization by RSM

RSM is a set of mathematical methods that relies on the experimental design to determine the range of independent input variables. It allows, using empirical mathematical models, to determine an approximation relation between the output responses and the input variables to optimize the physical parameters to achieve desirable responses.

RSM allows development a second-order polynomial model (Eq. 1) which includes the interactions between independent parameters (Xj) and the response (Y):

$$Y = \beta_0 + \sum_{J=1}^{P} \beta_j x_j + \sum_{J=1}^{P} \beta_{jj} x_j^2 + \sum_{i<j}^{P} \beta_{ij}\, x_i x_j \qquad (1)$$

Where; Y: Response function, β_o: Constant, β_j, β_{jj}, β_{ij}: Coefficients of the linear, quadratic, and interactive terms, respectively, x_j: Independent factors.

In the last decade, RSM has become a preferred and useful tool to optimize heterogeneous photocatalysis for wastewater treatment [17,21,32–35]. The most commonly used experimental designs are D-Optimal design, Box-Behnken design, Central Composite designs, and Doehlert matrix [17,19,21,36–38].

The D-optimal design was chosen in this study due to its simplicity, feasibility, efficiency, and minimal number of trials required. Additionally, D-optimal designs are used for multifactorial experiments with both quantitative and qualitative factors [32,39].

The experiments were designed with three quantitative factors (X1: catalyst dose, X2: DV 51 concentration and

Table 1: Factors type, their ranges and levels.

Quantitative factors			
	Range and levels		
	Low level (-1)	Central point (0)	High level (+1)
Catalyst dose (g/L) (X_1)	0.025	0.1125	0.2
DV 51 concentration (ppm) (X_2)	10	42.5	75
Reaction time (min) (X_3)	15	67.5	120
Qualitative factor			
Catalyst type (X_4)	ZnO	TiO_2	

X3: reaction time) and one qualitative factor (X4: catalyst type ZnO or TiO_2). The DV 51 photodegradation yield (R %) was selected as the response of the model; the factor levels are grouped in Table 1.

EXPERIMENTAL SECTION

Reagents and chemicals

$K_2Cr_2O_7$, C2H8N2O4, p-benzoquinone, and ter-butanol were of analytical quality used without any pre-treatment. Direct Violet 51 ($C_{32}H_{27}N_5Na_2O_8S_2$, MW = 719.7 g/mol) chosen as a model pollutant, was kindly provided by a textile company (Algiers); it is an anionic azo dye (purple powder) soluble in water. Two commercial catalysts were used namely ZnO (Sigma Aldrich) and TiO_2 P25 (Degussa-Evonik). Purified water was employed for preparing solutions.

Experimental procedure

The textile synthetic effluent was prepared by dissolving an accurate mass of DV 51 corresponding to the desired concentration in water. The required quantity of the catalyst was poured into 200 mL of the solution to be treated. An Erlenmeyer flask (200 mL), used as open reactor, was directly exposed to sunlight in a clear day (Fig. 1). The catalyst powder was recovered by using 0.45 µm hydrophobic PTFE Millipore filters. The analysis of the residual DV 51 concentration was realized by measuring its absorbance at the maximum peak (λ_{max} = 546 nm), thanks to a Shimadzu UV/Visible spectrophotometer. The absorbance is proportional to the pollutant concentration (Abs = ε l C), and the concentration was deduced by linear interpolation. ε is the molar extinction coefficient and l is the path length. The degradation yield R (%) is defined as follows:

$$R(\%) = \frac{C_0 - C_f}{C_0} \times 100 \qquad (2)$$

Fig. 1: Experimental set up used for solar degradation of DV 51.

C_o: pollutant initial concentration (ppm), C_f: pollutant final concentration (ppm)

RESULTS AND DISCUSSION

Preliminary tests

The preliminary tests consist in comparing the effectiveness of different processes with regard to the elimination of Direct Violet 51 as well as in selecting the parameters influencing the dye photodegradation.

To evaluate the real contribution of each process in the dye removal, tests of adsorption, photolysis and solar photocatalysis were carried out in the presence of ZnO and TiO_2 under the same conditions.

The results (Fig. 2) clearly show that adsorption and solar photolysis are ineffective for the DV 51 elimination with abatements of 1 and 8% respectively. On the other hand, the heterogeneous solar photocatalysis leads almost to a quasi-total degradation during the same time (160 min.).

The same trend was observed with TiO_2; the elimination of DV 51 is negligible by adsorption and photolysis while an abatement of 81% was obtained by photocatalysis for the same duration. Therefore, photocatalysis is chosen for water treatment polluted by DV 51.

Catalyst dose effect

To assess the effect of the catalyst dose on the DV 51 photodegradation, tests were performed with various doses between 0.025 and 0.5 g/L.

As expected, Fig. 3 shows that the degradation increases with augmenting dose. For a treatment of 30 min., rates of 24, 69, 85 and 96% are obtained respectively for doses of 0.025, 0.05, 0.1 and 0.25 g/L of ZnO. This proportionality is attributed to the augmentation of active sites of the catalyst and consequently to a higher concentration of reactive species which participate

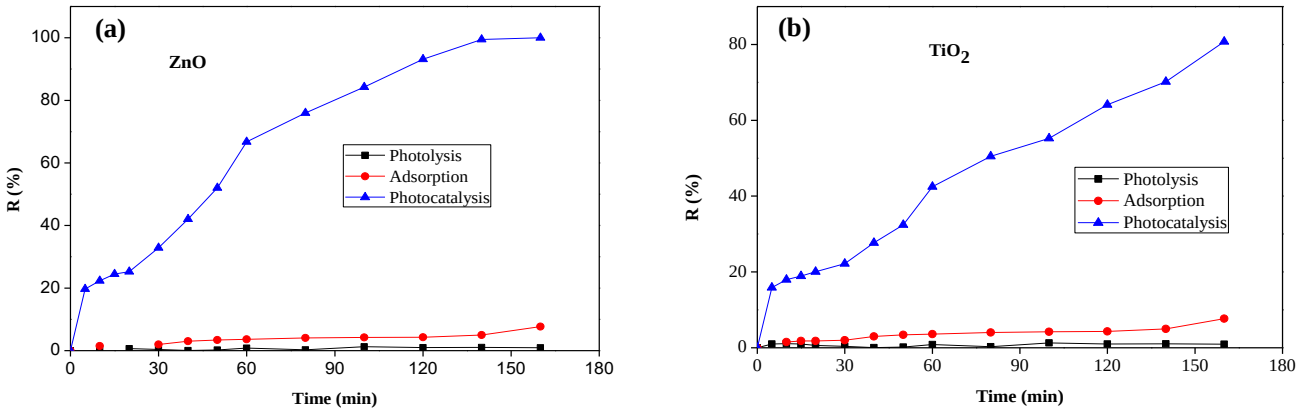

Fig. 2: Temporal evolution of DV 51 elimination efficiency using different processes in presence of a) ZnO, b) TiO_2

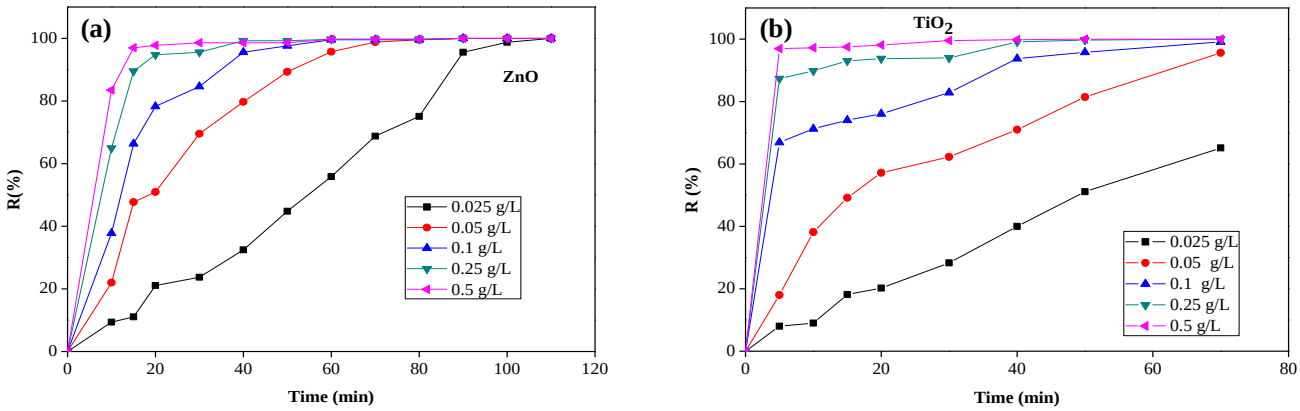

Fig. 3: Effect of the catalyst dose on the photodegradation efficiency of DV 51 using a) ZnO, b) TiO_2

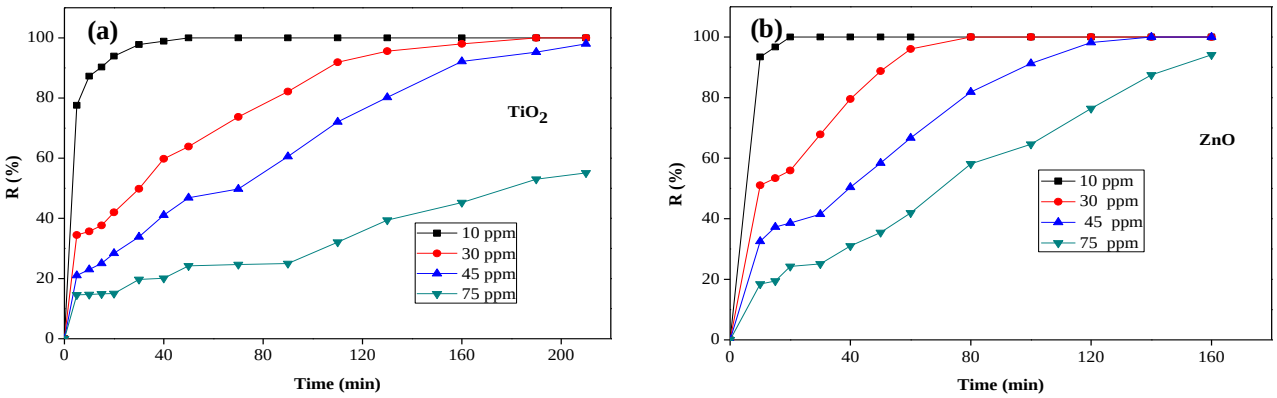

Fig. 4: Influence of the dye concentration Co on the photodegradation yield of DV 51 in presence of a) TiO_2, b) ZnO

photo-activity. Beyond 0.25 g/L, the efficacy remains nearly unchanged when the dose increases, and this is attributed to the high catalyst doses increasing the opacity and the turbidity of the solution, which attenuate the diffusion of the luminous flux (screening effect) [40].

The same behavior is observed for TiO_2; beyond 0.25 g/L, the photocatalytic efficiency remains unchanged.

Effect of DV 51 concentration

Real effluents contain dyes at concentrations as high as of 50 ppm and it is instructive to search the effect on the photocatalytic efficiency of the initial DV 51 concentration (C_O).

As expected, the photodegradation yield is inversely proportional to C_O. The best efficiency was reached at low

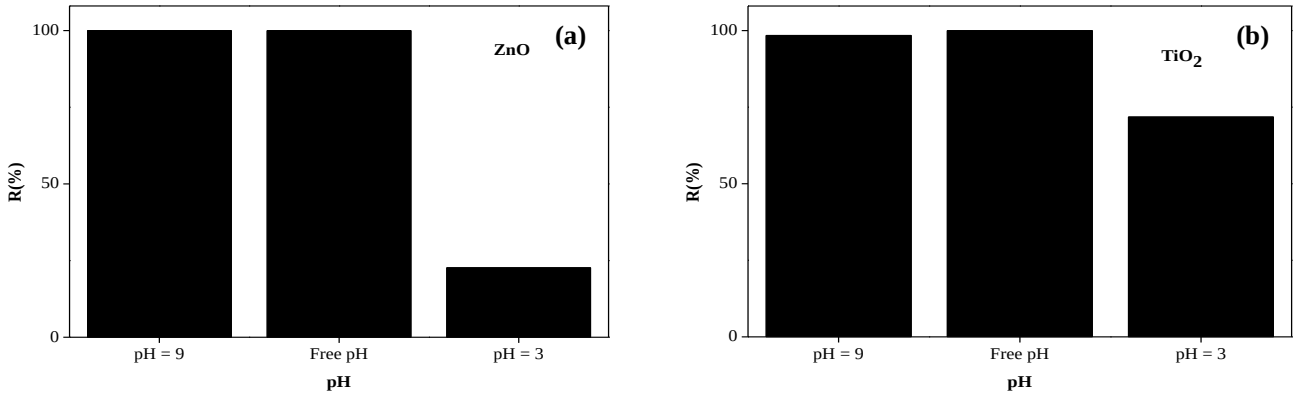

Fig. 5: pH-influence on the photocatalytic yield of DV 51 using a) ZnO b) TiO_2

concentration (10 ppm) with degradation rates of 100 and 98% under sunlight respectively for ZnO and TiO_2 after 30 and 40 min. On the other hand, only 25 and 20% were obtained for a concentration of 75 ppm for the same irradiation time.

This can be explained as follows: concentrated solutions lead to high number of dye molecules, which are adsorbed on the catalyst powder occupying the photo-electrochemical sites, which inhibits the formation of the reactive entities responsible for the photocatalysis. Moreover, the appearance of the screen effect is favored in the case of high concentrations, which reduces light penetration, which is essential for dye photodegradation and thereby decreases considerably the photoactivity.

pH effect

To investigate the effect of pH on DV 51 photodegradation, three pHs were tested namely 3, free and 9 using 0.025 g/L as catalyst dose.

At basic pH 9, the photocatalytic efficiency is not influenced and remains almost unchanged compared to that obtained for the free pH (without adjustment), for both photocatalysts ZnO and TiO_2 (Fig. 5). On the contrary, at acid pH (~ 3), a negative influence is observed, with a photodegradation yields of 24 and 72% respectively on ZnO and TiO_2 compared to a total degradation obtained at free pH. Following these results, the free pH is considered as optimal among all the range of pH studied. In addition, it is close to the natural environment without the addition of buffers.

Response surface methodology: D-Optimal model

The synthetic effluent loaded with DV 51 was treated under sunlight on ZnO or TiO_2 according to the RSM matrix. The experimental matrix and statistical combinations of four factors generated by D-Optimal design are grouped in Table 2 where 25 experiments were performed in accordance with the experimental protocol presented previously.

This approach produces a polynomial equation of second-order (Eq. 3) that have a relationship between the photocatalytic efficiency (R%) and the physical parameters, namely the catalyst dose (X_1), DV 51 concentration (X_2) and reaction time (X_3). R% is evaluated as the sum of a constant, three first-order effects (X_1, X_2 and X_3), three second-order effects (X_1^2, X_2^2 and X_3^2) and three interaction effects (X_1X_2, X_1X_3 and X_2X_3).

$$Y = 61.1203 + 15.0295\ X_1 - 29.7521\ X_2 + 13.086\ X_3 + 0.46909\ \begin{pmatrix} 1 \\ -1 \end{pmatrix} - 13.7322\ X_1^2 + 10.1799\ X_2^2 - 3.73099\ X_3^2 + 3.30977\ X_1 X_2 - 0.0344594\ X_1 X_3 + 2.55238\ X_1 \begin{pmatrix} 1 \\ -1 \end{pmatrix} + 2.40025\ X_2 X_3 + 2.605\ X_2 \begin{pmatrix} 1 \\ -1 \end{pmatrix} + 2.9189\ X_3 \begin{pmatrix} 1 \\ -1 \end{pmatrix} \quad (3)$$

For ZnO (+1):

$$Y = 61.58939 + 17.58188\ X_1 - 27.1471\ X_2 + 16.0049\ X_3 - 13.7322\ X_1^2 + 10.1799\ X_2^2 - 3.73099\ X_3^2 + 3.30977\ X_1 X_2 - 0.0344594\ X_1X_3 + 2.40025\ X_2 X_3 \quad (3.a)$$

For TiO_2 P25 (-1):

$$Y = 60.65121 + 12.47712\ X_1 - 32.671\ X_2 + 10.1671\ X_3 - 13.7322\ X_1^2 + 10.1799\ X_2^2 - 3.73099\ X_3^2 + 3.30977\ X_1 X_2 - 0.0344594\ X_1X_3 + 2.40025\ X_2 X_3 \quad (3.b)$$

Evaluation of the accuracy of the statistical model

Several methods allow evaluation the adequacy of a statistical model such as the difference between the predicted

Table 2: Design matrix with predicted and experimental values of DV 51 degradation yield (R%).

Run	X1	X2	X3	X4	Experimental values of R (%)	Predicted values of R (%)	Deviation
1	0.025	10	50	ZnO	75.73	65.95	9.77
2	0.025	75	85	ZnO	15.89	15.73	0.15
3	0.025	31.66	15	ZnO	11.969	22.58	-10.61
4	0.025	53.33	120	ZnO	36.421	34.36	2.05
5	0.2	10	85	ZnO	96.44	103.56	-7.12
6	0.2	75	50	ZnO	42.43	45.24	-2.81
7	0.2	53.3333	15	ZnO	41.139	38.12	3.01
8	0.2	31.6667	120	ZnO	91.5	85.95	5.54
9	0.1416	10	15	ZnO	89.05	84.82	4.22
10	0.0833	10	120	ZnO	97.33	102.51	-5.18
11	0.0833	75	15	ZnO	15.04	13.98	1.05
12	0.1416	75	120	ZnO	64.63	64.7	-0.09
13	0.025	10	15	TiO_2	62.5	68.75	-6.25
14	0.2	10	15	TiO_2	91.12	87.15	3.96
15	0.025	75	15	TiO_2	0.813	-7.37	8.19
16	0.2	75	15	TiO_2	18.37	24.26	-5.89
17	0.025	10	120	TiO_2	89.28	84.35	4.92
18	0.2	10	120	TiO_2	100	102.62	-2.62
19	0.025	75	120	TiO_2	10.97	17.82	-6.85
20	0.2	75	120	TiO_2	53.89	49.33	4.55
21	0.1125	42.5	67.5	TiO_2	60.128	60.65	-0.52
22	0.1125	42.5	67.5	TiO_2	61.041	60.65	0.38
23	0.1125	42.5	67.5	TiO_2	60.646	60.65	-0.005
24	0.1125	42.5	67.5	TiO_2	61.671	60.65	1.01
25	0.1125	42.5	67.5	TiO_2	59.77	60.65	-0.88

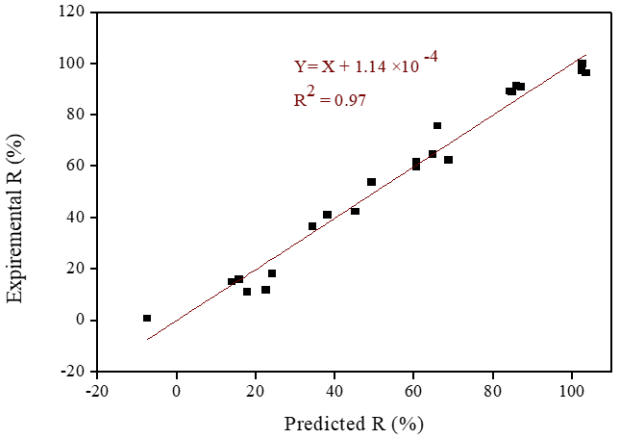

Fig. 6: Observed versus predicted photodegradation yield

and experimental responses, R^2, R^2_{adj}, Q^2 and the reproducibility [41–43].

Table 2 groups the experimental response (degradation yield) for 25 experimental tests and those predicted by calculation along with the relative error.

The obtained values of the coefficients R^2 and R^2_{adj} are respectively 0.97 and 0.94, thus revealing a good accord between the predicted values of the degradation efficiency and those observed experimentally (Fig. 6). Furthermore, the obtained value of the prediction coefficient ($Q^2 = 0.75$) indicates that the elaborated model fits suitably the experimental results [41].

The reproducibility is the variation in the response under the same conditions, often at center points, relative to the total variation in response. When the reproducibility value is close to 1, the pure error tends to 0 and this indicates that the response values are identical [MODDE 6.0]. A value of 0.99 (> 0.85) is obtained in this study, which produces a good reproducibility of the results.

Table 3: Statistical analysis of modeling results.

	Coefficient	P-value	Observation
1	15.03	5.69×10^{-6}	Significant
2	-29.75	5.52×10^{-9}	Significant
3	13.09	2.08×10^{-5}	Significant
4	0.47	0.76161	Not Significant
5	-0.47	0.76161	Not Significant
6	-13.73	0.00353	Significant
7	10.18	0.019253	Significant
8	-3.73	0.336955	Not Significant
9	3.31	0.143269	Not Significant
10	-0.03	0.987197	Not Significant
11	2.55	0.195494	Not Significant
12	-2.55	0.195494	Not Significant
13	2.40	0.277263	Not Significant
14	2.61	0.187127	Not Significant
15	-2.61	0.187127	Not Significant
16	2.92	0.143275	Not Significant
17	-2.92	0.143275	Not Significant

R^2 = 0.97, Adjusted R^2 = 0.94, Q^2 = 0.75 and Reproducibility = 0.99

ANOVA Analysis

ANOVA is an essential tool in determining the significance of a mathematical model [44]. A model is considered valid if the mean square of the regression is greater than the mean square of the residuals (MC regression > MC residual) [45]. Respective values of 1729.2 and 55.8 indicate that the model seems quite significant, thus confirming its validity. ANOVA represents the parameters for evaluating the adequacy of the model and is calculated using the MODDE 6.0 software (Table 3) [46].

Effects and interactions

Analyzing the factors and their interactions provides insight into how they influence the response. The graphical analysis (Fig. 7) shows that the DV 51 concentration (X2) has the most significant effect, evaluated at 59.50% (negative effect). Its increase inhibits the photoactivity; at larger concentrations, more dye molecules are adsorbed on the catalyst powder where the light penetration is weakened. Therefore, fewer photons reach the catalyst surface thus minimizing the photocatalytic efficiency.

By contrast, increasing the dose promotes the degradation efficiency, which has a positive effect of 30%. A high dose increases the active surface sites, thus augmenting the number of reactive radicals responsible for the photodegradation.

As expected, the reaction time (X3) has also a positive effect (26%) on the degradation and extending the treatment time improves photocatalytic degradation and also the mineralization as reported previously by [47].

Simplification of the RSM model

The p-value is used in order to simplify the photodegradation yield model, given by Eq. 1. If $p < 0.05$, the coefficient is significant and becomes insignificant beyond this value [48]. Table 3 presents the p-values corresponding to each coefficient of the model. Coefficients with p-values larger than 0.05 are removed and the general model Eq. (3) becomes:

$$Y = 60.0412 + 14.9039\ X_1 - 29.6789\ X_2 + 12.8966\ X_3 + 0.396841 \begin{pmatrix} 1 \\ -1 \end{pmatrix} - 14.7797\ X_1^2 + 9.13245\ X_2^2 \quad (4)$$

$$Y_{ZnO} = 60.4380 + 14.9039\ X_1 - 29.6789\ X_2 + 12.8966\ X_3 - 14.7797\ X_1^2 + 9.1324\ X_2^2 \quad (4.a)$$

$$Y_{TiO2} = 59.6444 + 14.9039\ X_1 - 29.6789\ X_2 + 12.8966\ X_3 + - 14.7797\ X_1^2 + 9.1324\ X_2^2 \quad (4.b)$$

Validation of the simplified model using the test points

To validate the simplified model, the points which were not used must be added. Therefore, eight additional new experiments were performed as part of the field study.

The selected validation points, the experimental and predicted responses as well as the deviation between them are illustrated in Table 4. The latter shows that the difference between the experimental values and those predicted is small. This means that the predictions are good and the model is validated.

For clarity and easy understanding of the validation, the predicted values using the simplified model as well as the photodegradation yields are illustrated in Fig. 8. The measured values are plotted and their proximity to the ideal line (bisector) confirms the validity of the model, considered as accurate when all measured values are aligned or close to the ideal line. According to the validation test, it can be concluded that the simplified model is well validated.

Table 4: Simplified model's validation dataset and comparison between predicted and experimental results

Experiment	X_1	X_2	X_3	X_4	Experimental values of R (%)	Predicted values of R (%)	Deviation
26	0.5	0.5	0.5	ZnO	54.79	59.41	4.62
27	0.5	0.5	-0.5	ZnO	45.46	46.33	0.87
28	0.5	-0.5	0.5	ZnO	89.79	89.17	-0.62
29	-0.5	0.5	0.5	ZnO	42.21	44.38	2.17
30	-0.5	-0.5	0.5	ZnO	76.43	74.14	-2.29
30	-0.5	-0.5	-0.5	ZnO	68.62	61.05	-7.57
31	0.5	0.5	0.5	TiO_2	49.13	59.41	10.28
32	0.5	0.5	-0.5	TiO_2	39.27	46.33	7.06
33	0.5	-0.5	0.5	TiO_2	87.18	89.17	1.99
34	-0.5	0.5	0.5	TiO_2	37.49	44.38	6.89
35	-0.5	-0.5	0.5	TiO_2	72.63	74.14	1.51
36	-0.5	-0.5	-0.5	TiO_2	61.88	61.05	-0.83

R^2 = 0.948. Ajusted R^2 = 0.931. Q^2 = 0.891

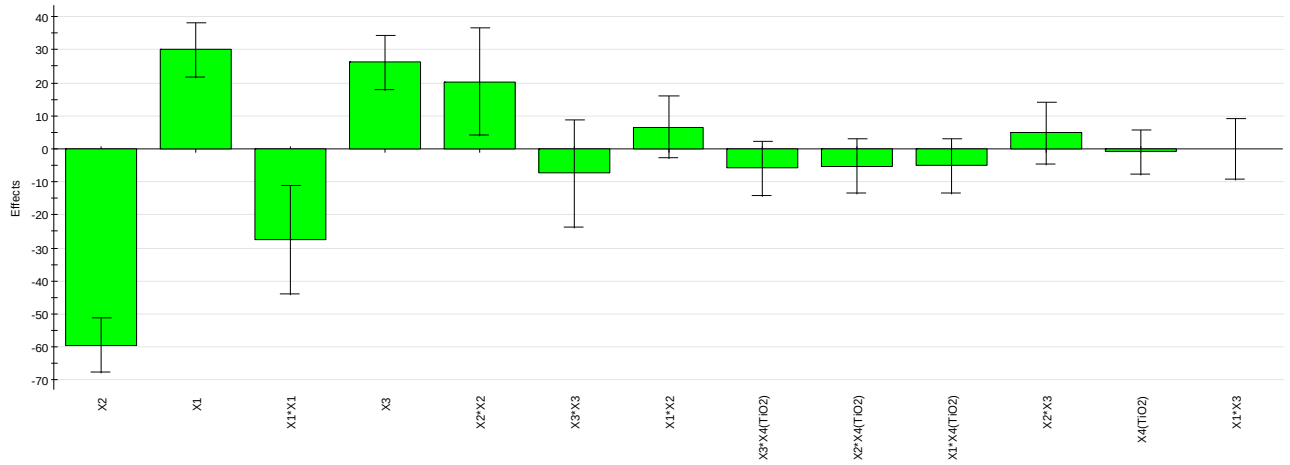

Fig. 7: Graphical analysis of factors effect and their interactions

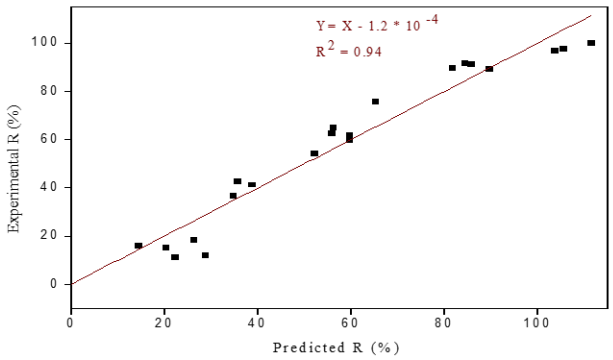

Fig. 8: Validation of the simplified model

Response surface analysis

The graphical illustration of the results is a simple method to optimize and identify the interactions between the physical factors. Each curve represents an infinity of combinations between two factors when the third is maintained constant.

Catalyst dose constant

The interaction between the DV 51 concentration (C_O) and the reaction time for fixed catalyst doses (0.025, 0.141, and 0.2 g/L) show that the photodegradation yield (R%) decreases with increasing C_O (Fig. 9) while the increase of the reaction time favors the DV 51 photodegradation for both ZnO and TiO_2.

Indeed, using TiO_2 and for the same value of X_2 = 65 ppm, the passage from 25 to 85 min increases the degradation yield from 2 to 20%, 30 to 48%, and 32 to 48%, respectively for doses of 0.025, 0.141 and 0.2 g/L.

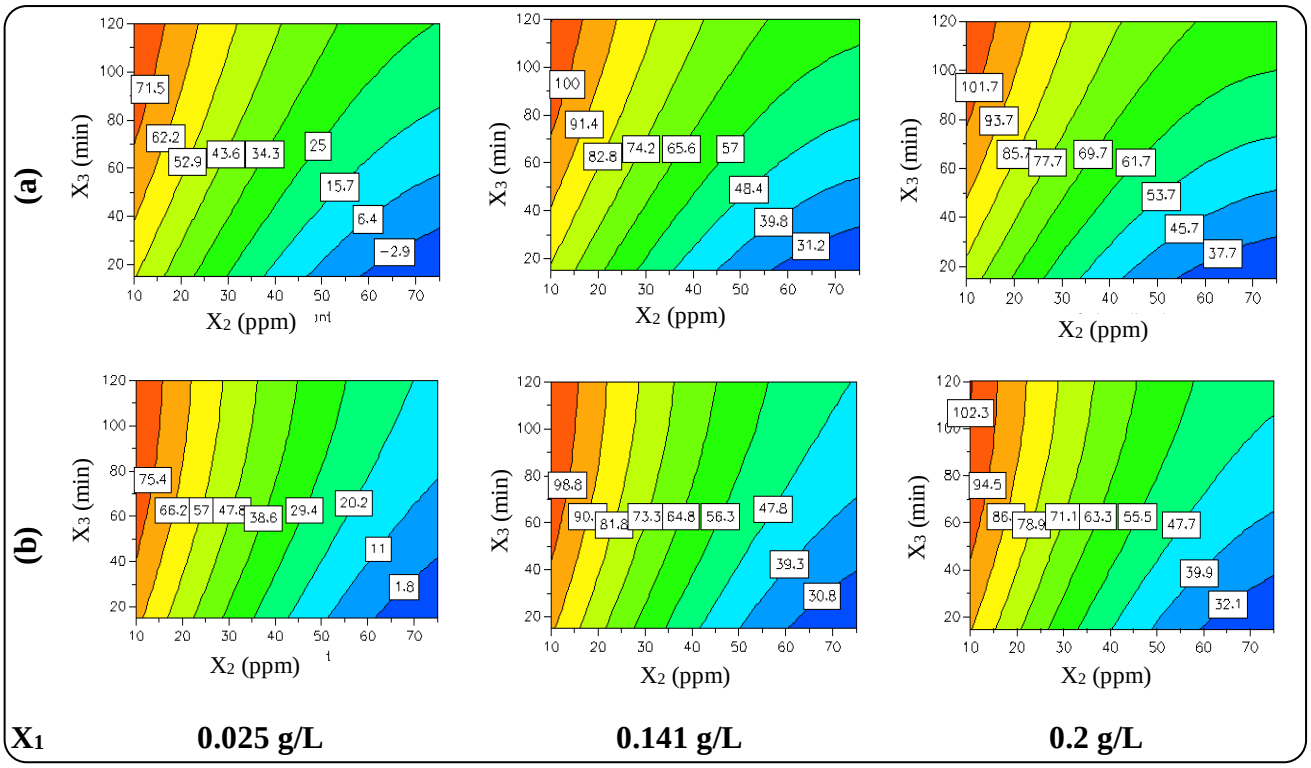

Fig. 9: Response surface plot indicating the interaction between X_2 (DV 51 concentration) and X3 (Reaction time) with X_1 (Catalyst dose) fixed at lower, center and higher levels for a) ZnO b) TiO_2

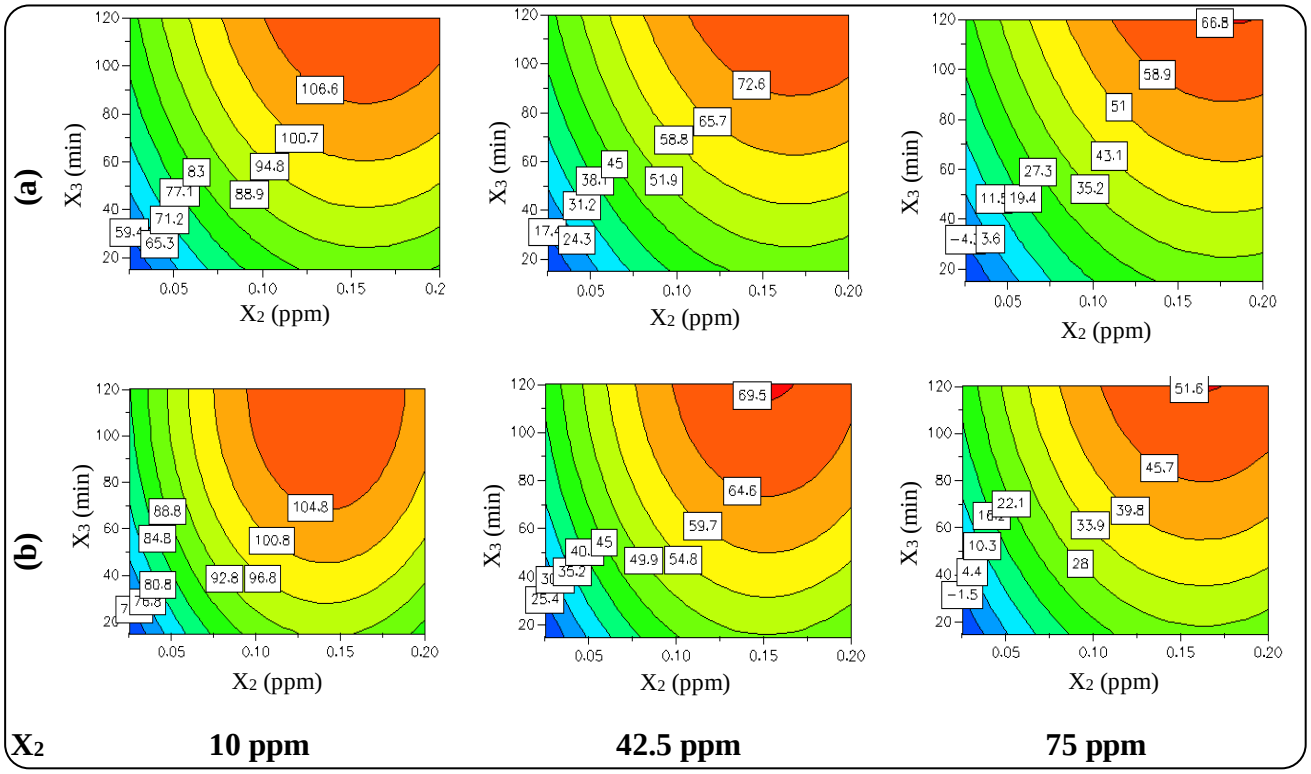

Fig. 10: Response surface plot indicating the interaction between X_1 (Catalyst dose) and X_3 (Reaction time) with X_2 (DV 51 concentration) fixed at lower, center and higher levels for a) ZnO b) TiO_2

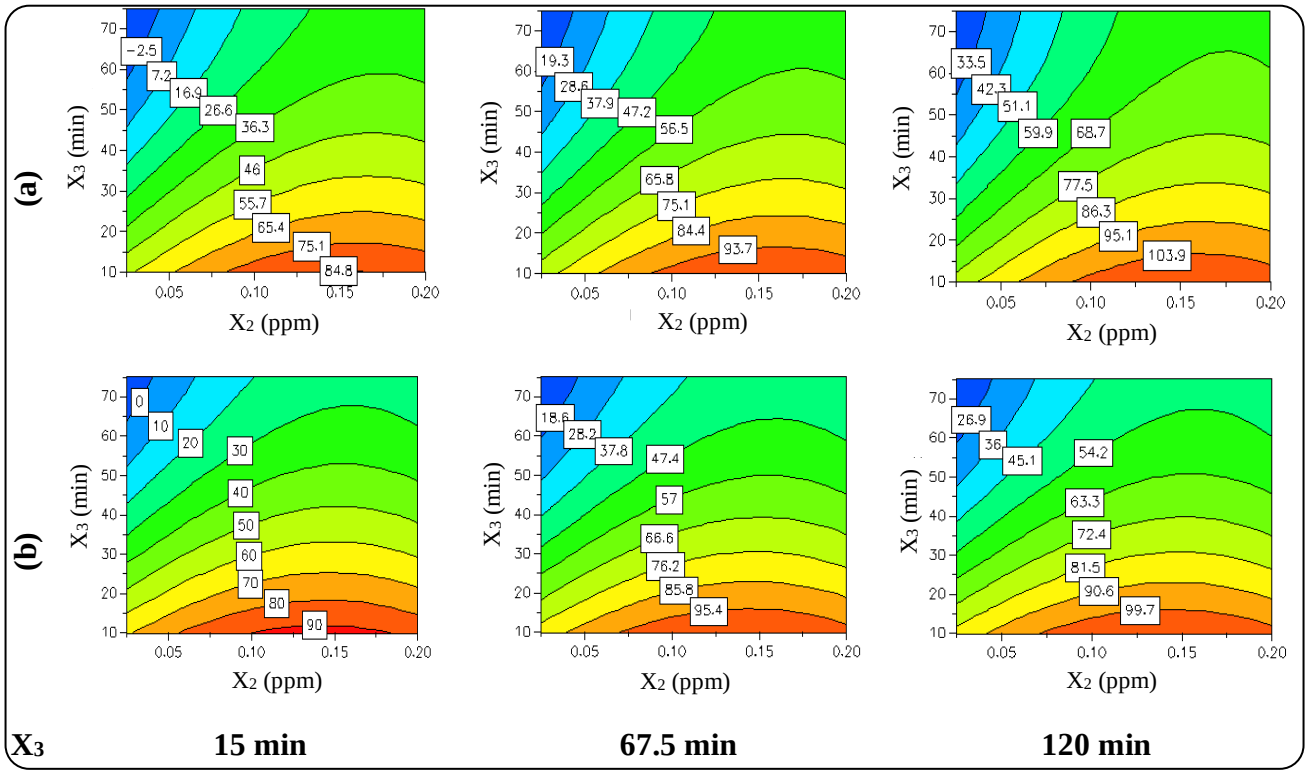

Fig. 11: Response surface plot indicating the interaction between X_1 (Catalyst dose) and X_2 (DV 51 concentration) with X_3 (Reaction time) fixed at lower, center and higher levels for a) ZnO b) TiO_2

DV 51 concentration constant

The interaction between the catalyst dose and the reaction time (Fig. 10) reveal that the degradation augments with augmenting both the catalyst dose and reaction time, and this is valid for ZnO and TiO_2.

Reaction time constant

The interaction between the DV 51 concentration (C_O) and the catalyst dose (Fig. 11) shows that the effect of the catalyst dose on the photoactivity is positive; for the same value of X2, increasing the dose improves the photodegradation. As example, for X2 = 15 ppm, the variation of the catalyst dose from 0.05 to 0.15 g/L augments the photocatalytic rate from 56 to 75%, 75 to 94% and 81 to 100% respectively for reaction time of 15, 67.5 and 120 min. This behavior is reproduced for both ZnO and TiO_2.

Prediction of optimal conditions for DV 51 photodegradation

The optimal conditions given by the MODDE Software, corresponding to the maximal photodegradation yield are grouped in Table 5. The highest degradation efficiency of DV 51 using ZnO happening at conditions of catalyst dose of 0.1567 g/L, C_O of 10 ppm and reaction time of 120 min.

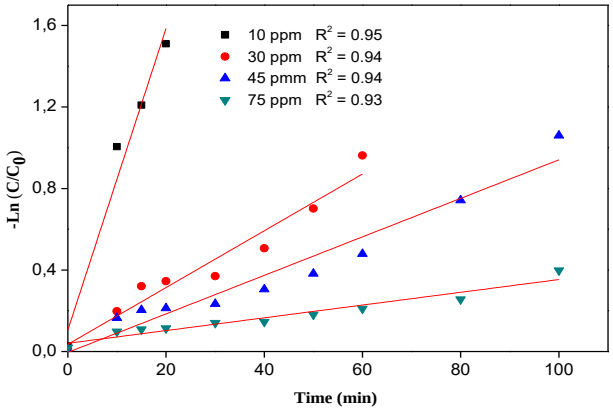

Fig. 12: Kinetic model of the DV 51 photodegradation by [ZnO] ([ZnO] = 0.1 g/L, solar photocatalysis at natural pH)

Kinetic study of DV 51 removal by ZnO

The knowledge of the kinetic order of the DV 51 photo-reaction, is determined from the curves –ln (C/C_o) versus the illumination time for different concentrations C_O (Fig. 12). The linear regression of these curves provides straight lines that pass by the origin with high regression

Table 5: Predicted values of optimal conditions for DV 51 photodegradation

X1 (g/L)	X2 (ppm)	X3 (min)	X4	R (%)
0.1567	10	120	ZnO	100
0.1678	42.5	120	ZnO	84.6
0.1792	75	120	ZnO	76.79
0.1417	10	120	TiO_2	100
0.1521	42.5	120	TiO_2	72.58
0.1627	75	120	TiO_2	44.52

coefficients (R^2), indicating a pseudo-first order kinetic for the DV 51 photo-reactions.

The Langmuir-Hinshelwood (L-H) kinetic model is based on the hypothesis that the pollutants molecules are physically adsorbed onto the surface of catalysts. It is largely used to describe the kinetics of the pollutants photodegradation and permits to evaluate the DV 51 degradation rate using ZnO at different initial concentrations:

$$\frac{1}{k_{app}} = \frac{1}{k_r} C_o + \frac{1}{k_r K} \quad (5)$$

With: k_{app}: The apparent kinetic constant of the pseudo-first order reaction (min^{-1}), k_r: The specific rate constant (mg/L.min), K: The adsorption equilibrium constant (L/mg).

The plot ($1/K_{app}$) as a function of C_O (Fig. 13) is linear with a correlation coefficient R^2 of 0.99 with values of k_r and K equal respectively to 0.35 mg/L min^{-1} and - 0.13 L mg^{-1}. The results indicate that the L-H model is suitable to describe the DV 51 photodegradation process.

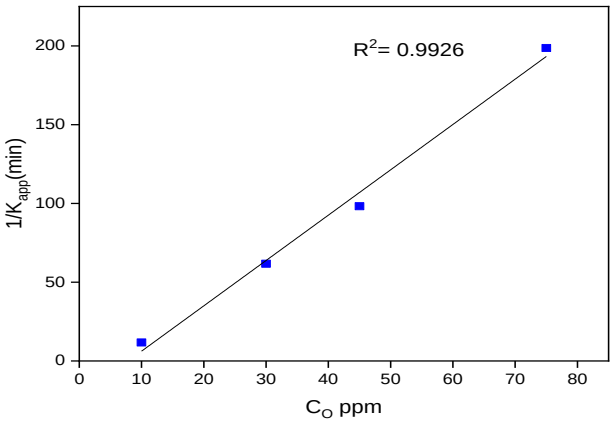

Fig. 13: Kinetic parameters of L-H model ([ZnO] = 0.1 g/L, solar light at natural pH)

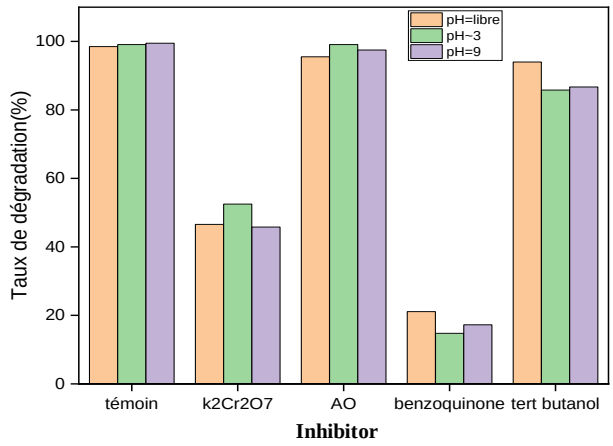

Fig. 14: Effect of different scavengers on DV 51 photodegradation (Co = 42.5 ppm, [ZnO] = 0.16 g/L and 120 min)

Dye photo-degradation mechanism

When a photocatalyst is exposed to solar or artificial radiations, active species are generated, namely: electrons (e^-), holes (h^+), superoxide ($^\bullet O_2^-$), and hydroxyl ($^\bullet OH$). The photo-oxidation can occur by the action of one or more reactive species.

The identification of the active species implicated in the photo-reaction is a decisive step in proposing a reaction mechanism for the DV 51 oxidation. The use of scavengers is an indirect method to achieve this goal; it consists of trapping the radicals with an appropriate inhibitor (scavenger) and then monitoring the kinetics of the photo-degradation.

For the photodegradation of DV 51 on ZnO, the role of reactive species: e^-, h^+, $O^\bullet{}_2^-$ and $^\bullet OH$ was demonstrated by the following inhibitors: $K_2Cr_2O_7$ (0.6 mmol/L), $(NH_4)_2C_2O_4$ (0.6 mmol/L), benzoquinone (0.6 mmol/L) and ter-butanol (0.1 mol/L) respectively. For each pH value (3, free and 9), five experiments were carried out simultaneously. The four inhibitors were added to the four solutions while the fifth was considered as a control sample. The C_o concentration was kept at 42.5 ppm and the catalyst dose at 0.16 g/L under solar radiation within 120 min.; the obtained results are illustrated in Fig. 14.

By adding $(NH_4)_2C_2O_4$ or ter-butanol, the photodegradation was not influenced, which clearly indicates that h^+ and $^\bullet OH$ are not involved in the DV 51 degradation.

On the other hand, significant inhibition of 79 % (i.e. only 21% of degradation) and 54% (i.e., only 46% of degradation) were obtained respectively after the addition of benzoquinone and $K_2Cr_2O_7$.

In light of these results, the superoxide $O^\bullet{}_2^-$ and e^- are the principal species responsible for the DV 51 photodegradation and this is valid for all pHs and a reaction mechanism has been suggested:

Table 6: Comparison between the optimal removal efficiency of DV 51 reported in literature.

N°	Author	Technique	Material/Reactor design	Degradation yield of DV 51	Ref.
01	Boutra et al.	Solar photocatalysis	TiO_2/Batch ZnO/Batch	100 % 97 %	Current study
02	Yavuz et al. (2015)	Electrochemical method	Graphite electrodes/ Batch	94 %	[14]
03	Loganathan et al. (2019)	Solar / UV photocatalysis	CeO_2-rGO/ Batch	93 %	[22]
04	Vitor et al. (2008)	Biological	Candida albicans/ Batch	87 %	[38]
05	Enayatzamir et al. (2010)	Biotechnological	Phanerochaete chrysosporium/ immobilised into alginate beads	85 %	[37]
06	Byberg et al. (2012)	Photocatalysis	TiO_2 /Fixed bed	82 %	[5]
07	Sadaf et al. (2015)	Biosorption	Sugarcane bagasse/ Batch	60 %	[13]
08	Utara et al. (2014)	Adsorption	Natural Rubber Chips/ Batch	80 %	[15]

$$ZnO + h\nu \rightarrow ZnO\ (h^{+}_{BV} + e^{-}_{BC}) \quad (6)$$

$$O_{2ads} + e^{-}_{BC} \rightarrow O^{\bullet}_{2}{}^{-} \quad (7)$$

$$VD\ 51 + O^{\bullet}_{2}{}^{-} \rightarrow \text{by-products} \rightarrow CO_2 + H_2O + \text{mineral salts} \quad (8)$$

Comparison with previous studies

It is instructive at the level to make a comparison with the works in the open literature. Table 6 summarizes the optimal removal efficiency of DV 51 on different materials, and clearly shows the high performance of the solar photocatalysis compared to other processes.

Energy efficiency metrics

AOPs are costly in that the electric energy consumption presents a major fraction of the operating cost [49–51]. Generally, the kinetic rate constant enabled to calculation the efficacy of the system in terms of organic pollutant removal. However, for practical applications of AOPs, the performance metrics based on energy consumption must be taken into consideration because the most important design parameter of such systems is the amount of energy used to generate enough oxidizing agents. IUPAC recommended the utilization of standard figures of merit for the comparison of energy requirements regardless the nature of the AOP system [52]. For low contaminant concentrations, the figure of merit is "electric energy per order, $\left(E_{E0}, \frac{KWh}{m^3 order}\right)$" for electrically driven systems and "collector area per order, $(A_{CO}, \frac{m^2}{m^3 order})$" for solar-driven systems. E_{E0} is the electric energy necessary to reduce the contaminant concentration by one order of magnitude in the unit volume of water. For solar-driven systems, there is no cost for solar radiation A_{CO} which is the collector surface needed to achieve one order magnitude degradation of a contaminant per unit of volume of water receiving an average solar radiation $\overline{E_s}$. When The degradation kinetic is well described by first order kinetic, E_{EO} and A_{CO} can be calculated for batch reactor from Eq. (9) and Eq. (10), respectively [53,54]:

$$E_{EO} = \frac{t * P * 1000}{V * 60 * \log\left(\frac{C_i}{C_f}\right)} \quad (9)$$

$$A_{CO} = \frac{A_r * t * \overline{E_s}}{V * \log\left(\frac{C_i}{C_f}\right)} \quad (10)$$

Where: P: Electric power (kW), V: Volume of treated water (L), t: Time of treatment (min), A_r: The collector area (m^2), $\overline{E_s}$: The average solar radiation (W/m^2), C_i: The initial substrate concentration (mol/L), C_f: The final substrate concentration (mol/L)

In this section, the energy consumption of solar/ZnO and solar/TiO_2 systems for DV 51 removal were calculated. The appropriate figure of merit for this case is the collector area per order. In addition, for both catalysts, the DV 51 degradation have been performed under artificial UV light using three 18 W UV lamps. The results of these experiments served to evaluate the electric energy per order of both systems (UV/TiO_2 and UV/ZnO). The E_{E0} and A_{CO} for different systems-are summarized in Table 7.

Under artificial light, ZnO led to E_{E0} value of 256.00 $\frac{KWh}{m^3} order$, which represents lower electric consumption than the system UV/TiO_2. Under solar light, the collector area per order obtained for ZnO photocatalysis is lower than that for the system UV/TiO_2.

Table 7: Kinetic rates, electric energy per order, collector area per order and efficiency in energy use for different photocatalytic systems.

	Artificial UV light		Solar light	
Catalyst type	k_1 (min^{-1})	E_{E0} KWh/m^3 order	k_2 (min^{-1})	A_{CO} m^2/m^2 order
ZnO	0.0162	256.00	0.0174	127.73
TiO_2	0.0042	987.43	0.0086	258.43
Efficiency (%) [55]	74		50	

k_1: first order kinetic rate under artificial light, k_2: first order kinetic rate under solar light, C_O = 75 ppm, free pH and catalyst dose = 0.2 g/L, $\varepsilon_{UV} = \frac{E_{EO(TiO2)} - E_{EO(ZnO)}}{E_{EO(TiO2)}}$. $\varepsilon_{solar} = \frac{A_{CO(TiO2)} - A_{CO(ZnO)}}{A_{CO(TiO2)}}$

These results confirmed that in all experiments, ZnO utilized the introduced light more efficiently than TiO_2. The higher efficiency in the use of energy ($\varepsilon > 50$ %) demonstrated the performance of ZnO photocatalytic system to remove DV 51 both under solar and artificial light.

CONCLUSIONS

The current study provided an experimental and numerical contribution to the elimination by solar photocatalysis of a textile azo dye, namely Direct Violet 51. The experimental section studied the effect of various operational parameters on the efficiency of the DV 51 elimination under sunlight. Preliminary studies revealed that photocatalysis is among the most efficient processes for DV 51removal compared to adsorption and photolysis. The current work showed that the DV 51 degradation obeys a pseudo first-order kinetic model and the L-H model is suitable to describe the photoactivity. The use of RSM to optimize the DV 51 degradation revealed a slight interaction between the different parameters; it showed that the initial concentration of DV 51 has the large influence on the elimination efficiency, followed by the effect of catalyst dose and reaction time. The values of R^2 and R_{adj}^2 showed that the polynomial model is reliable. The estimation of E_{EO} and A_{CO} confirmed that ZnO photocatlysis used energy more efficiently under both solar and artificial light. The higher efficiency in the use of energy of this system is useful information and a key parameter for its large-scale implementation.

The DV 51 photo-degradation mechanism with ZnO indicates that $O^{\bullet}_2^-$ and e^- are the principal species involved in the DV 51 oxidation under solar radiation. Solar photocatalysis is an effective, simple, and clean treatment to reduce the toxicity of water polluted by dyes while limiting the energy cost of the treatment.

Acknowledgments

The authors are thankful to Miss S. Mahieddine and Mrs W. Yazid for their technical assistance. This work was supported financially by Unité de Développement des Equipements Solaires, UDES/Centre de Développement des Energies Renouvelables, CDER.

Received : Jun. 19, 2023 ; Accepted : Sep. 11, 2023

REFERENCES

[1] Byberg R., Cobb J., Martin L.D., Thompson R.W., Camesano T.A., Zahraa O., Pons M.N., Comparison of Photocatalytic Degradation of Dyes in Relation to their Structure, *Environ. Sci. Pollut. Res.*, **20:** 3570–3581 (2013).

[2] Igoud S., Zeriri D., Aoudjit L., Boutra B., Sebti A., Khene F., Mameche A., Climate Change Adaptation by Solar Wastewater Treatment (SOWAT) for Reuse in Agriculture and Industry, *Irrig. and Drain.*, **70:** 243–253 (2021).

[3] Tahir M.B., Tufail S., Ahmad A., Rafique M., Iqbal T., Abrar M., Nawaz T., Khan M.Y., Ijaz M., Semiconductor Nanomaterials for the Detoxification of Dyes in Real Wastewater under Visible-Light Photocatalysis, *International Journal of Environmental Analytical Chemistry*, **101:** 1735–1749 (2021).

[4] Laib R., Amokrane-Nibou S., Dahdouh N., Mansouri T.E.M., Removal of the Cationic Textile Dye by Recycled Newspaper Pulp and Its Cellulose Microfibers Extracted: Characterization, Release, and Adsorption Studies, *Iran. J. Chem. Chem. Eng.(IJCCE)*, **40:** 133–141 (2021).

[5] Bailey K., Basu A., Sharma S., The Environmental Impacts of Fast Fashion on Water Quality: A Systematic Review, *Water*, **14:** 1073 (2022).

[6] Barkat A., Bouaicha F., Mester T., Debabeche M., Szabó G., Assessment of Spatial Distribution and Temporal Variations of the Phreatic Groundwater Level Using Geostatistical Modelling: The Case of Oued Souf Valley—Southern East of Algeria, *Water*, **14:** 1415 (2022).

[7] Berradi M., Hsissou R., Khudhair M., Assouag M., Cherkaoui O., El Bachiri A., El Harfi A., Textile Finishing Dyes and their Impact on Aquatic Environs, *Heliyon*, **5:** e02711 (2019).

[8] Igoud S., Zeriri D., Boutra B., Mameche A., Benzegane Y., Belloula M., Benkara L., Aoudjit L., Sebti A., Compared Efficiency of Sustainable and Conventional Treatments of Saline Oily Wastewater Rejected by Petroleum Industry in Algerian Sahara, *Petroleum Science and Technology*, **40:** 92–106 (2022).

[9] Paździor K., Bilińska L., Ledakowicz S., A Review of the Existing and Emerging Technologies in the Combination of AOPs and Biological Processes in Industrial Textile Wastewater Treatment, *Chemical Engineering Journal*, **376:** 120597 (2019).

[10] UN Water, ed., "Groundwater Making the Invisible Visible", UNESCO, Paris, (2022).

[11] Azimi S.C., Shirini F., Pendashteh A.R., Advanced Oxidation Process as a Green Technology for Dyes Removal from Wastewater: A Review, *Iran. J. Chem. Chem. Eng. (IJCCE)*, **40(5):** 1467-1489 (2021).

[12] Furferi R., Volpe Y., Mantellassi F., Circular Economy Guidelines for the Textile Industry, *Sustainability*, **14(17):** 11111 (2022).

[13] Ribul M., Lanot A., Tommencioni Pisapia C., Purnell P., McQueen-Mason S.J., Baurley S., Mechanical, Chemical, Biological: Moving Towards Closed-Loop Bio-Based Recycling in a Circular Economy of Sustainable Textiles, *Journal of Cleaner Production*, **326:** 129325 (2021).

[14] Sadaf S., Bhatti H.N., Arif M., Amin M., Nazar F., Sultan M., Box–Behnken Design Optimization for the Removal of Direct Violet 51 dye from Aqueous Solution Using Lignocellulosic Waste, *Desalination and Water Treatment*, **56:** 2425–2437 (2015).

[15] Sürme Y., Demirci O., Determination of Direct Violet 51 Dye in Water Based on its Decolorisation by Electrochemical Treatment, *Chemical Papers*, **68:** 1491-1497 (2014).

[16] Utara S., Phataib P., Adsorption Characteristics of Direct Violet Dye by Natural Rubber Chips, *AMR*, **844:** 391–394 (2013).

[17] Assassi M., Madjene F., Harchouche S., Boulfiza H., Modeling and Optimization of the Photocatalytic Degradation of Tartrazine in Aqueous Solution, *Acta per Tech*, **52:** 133–145 (2021).

[18] Madjene F., Assassi M., Benhabiles O., Yeddou-Mezenner N., Optimisation and Kinetic Modelling of Atenolol Degradation by ZnO under Solar Irradiation, *International Journal of Environmental Analytical Chemistry*, **103:** 6675-6686 (2021).

[19] Mohammed N., Palaniandy P., Shaik F., Pollutants Removal from Saline Water by Solar Photocatalysis: a Review of Experimental and Theoretical Approaches, *International Journal of Environmental Analytical Chemistry*, **103(16):** 4155-4175 (2021).

[20] Pérez-Lucas G., Aatik A.E., Aliste M., Navarro G., Fenoll J., Navarro S., Removal of Contaminants of Emerging Concern from a Wastewater Effluent by Solar-Driven Heterogeneous Photocatalysis: A Case Study of Pharmaceuticals, *Water Air Soil Pollut*, **234:** 55 (2023).

[21] Thabet R.H., Fouad M.K., El Sherbiney S.A., Tony M.A., Solar Assisted Green Photocatalysis for Deducing Carbamate Insecticide from Agriculture Stream into Water Reclaiming Opportunity, *International Journal of Environmental Analytical Chemistry*, **104(4):** 938-960 (2022).

[22] Ramandi S., Entezari Mohammad H., Ghows N., Solar Photocatalytic Degradation of Diclofenac by N-Doped TiO_2 Nanoparticles Synthesized by Ultrasound, *Iranian Journal Chemistry and Chemical Engineering (IJCCE)*, **39:** 159–173 (2020).

[23] Brahimi R., Bessekhouad Y., Trari M., Physical Properties of N_xTiO_2 Prepared by Sol–Gel Route, *Physica B: Condensed Matter*, **407:** 3897–3904 (2012).

[24] Chekir N., Tassalit D., Benhabiles O., Kasbadji Merzouk N., Ghenna M., Abdessemed A., Issaadi R., A Comparative Study of Tartrazine Degradation Using UV and Solar Fixed Bed Reactors, *International Journal of Hydrogen Energy*, **42(13):** 8948-8954 (2016).

[25] Djilali M.A., Mellal M., Mekatel H., Belabed C., Mahieddine A., Boudiaf S., Trari M., Synthesis, Physical, Optical and Electrochemical Properties of the Ilmenite $CrFeO_3$: Application to Photo-Reduction of Ni^{2+}, *International Journal of Hydrogen Energy*, **47:** 1589–1604 (2022).

[26] Sharma A., Thuan D.V., Pham T.-D., Tung M.H.T., Truc N.T.T., Vo D.-V.N., Advanced Surface of Fibrous Activated Carbon Immobilized with FeO/TiO_2 for Photocatalytic Evolution of Hydrogen under Visible Light, *Chem. Eng. Technol*, **43:** 752–761 (2020).

[27] Byberg R., Cobb J., Martin L.D., Thompson R.W., Camesano T.A., Zahraa O., Pons M.N., Comparison of Photocatalytic Degradation of Dyes in Relation to their Structure, *Environ. Sci. Pollut. Res*., **20:** 3570–3581 (2013).

[28] Loganathan A., Sivakumar A., Murugesan B., Sivakumar P., Solar Light Active CeO_2/RgO Hybrid Photocatalyst for Direct Violet 51 Degradation, *RJC*, **12:** 1710–1724 (2019).

[29] Akhtar A., Hanif M., Rashid U., Bhatti I., Alharthi F., Kazerooni E., Advanced Treatment of Direct Dye Wastewater Using Novel Composites Produced from Hoshanar and Sunny Grey Waste, *Separations*, **9:** 425 (2022).

[30] Vitor V., Corso C.R., Decolorization of Textile Dye by Candida Albicans Isolated from Industrial Effluents, *J. Ind. Microbiol. Biotechnol*., **35:** 1353–1357 (2008).

[31] Enayatzamir K., Alikhani H.A., Yakhchali B., Tabandeh F., Rodríguez-Couto S., Decolouration of Azo Dyes by Phanerochaete Chrysosporium Immobilised into Alginate Beads, *Environ. Sci. Pollut. Res*., **17:** 145–153 (2010).

[32] Boutra B., Sebti A., Trari M., Response Surface Methodology and Artificial Neural Network for Optimization and Modeling the Photodegradation of Organic Pollutants in Water, *Int. J. Environ. Sci. Technol*., **27(27):** 34018-34036 (2022).

[33] Kaur M., Noonia A., Dogra A., Singh Thind P., Optimising the Parameters Affecting Degradation of Cypermethrin in an Aqueous Solution Using TiO_2 /H_2O_2 Mediated UV Photocatalysis: RSM-BBD, Kinetics, Isotherms and Reusability, *International Journal of Environmental Analytical Chemistry*, **103(5):** 1153-1167 (2021).

[34] Khamis Abadi M.R., Feizbakhsh A., Ahmad Panahi H., E. Konoz, Synthesis and Characterisation of Zinc Oxide-Chromium Oxide for Optimisation of Photocatalytic/H_2O_2 Process by Response Surface Methodology: Selective and Regeneration Studies, *International Journal of Environmental Analytical Chemistry*, **103(15):** 3634-3647 (2021).

[35] Mohammadi Azar D., Feizbakhsh A., Panahi H.A., Niazi A., Fabrication of the Novel CoS_2/ZnO Nanocomposites with Photocatalysis Properties and Response Surface Methodology Study, *International Journal of Environmental Analytical Chemistry*, **102(19):** 8490-8502 (2020).

[36] Berkani M., Kadmi Y., Bouchareb M.K., Bouhelassa M., Bouzaza A., Combinatıon of a Box-Behnken Design Technique with Response Surface Methodology for Optimization of the Photocatalytic Mineralization of C.I. Basic Red 46 Dye from Aqueous Solution, *Arabian Journal of Chemistry*, **13(11):** 8338–8346 (2020).

[37] Thabet R.H., Fouad M.K., Ali I.A., El Sherbiney S.A., Tony M.A., Magnetite-Based Nanoparticles as an Efficient Hybrid Heterogeneous Adsorption/Oxidation Process for Reactive Textile Dye Removal from Wastewater Matrix, *International Journal of Environmental Analytical Chemistry*, **103(11):** 2636-2658 (2021).

[38] Moslemzadeh M., Khaghani R., Salarian A., Esrafili A., Synthesis of New Catalyst Based on TiO_2 Immobilised in Steel Slag for Photocatalytic Degradation of Permethrin in Aqueous Solutions: RSM Method, *International Journal of Environmental Analytical Chemistry*, 1–20 (2022).

[39] Zahmatkesh S., Far S.S., Sillanpää M., RSM-D-Optimal Modeling Approach for COD Removal from Low Strength Wastewater by Microalgae, Sludge, and Activated Carbon- Case Study Mashhad, *Journal of Hazardous Materials Advances*, **7:** 100110 (2022).

[40] Herrmann J.-M., Photocatalysis Fundamentals Revisited to Avoid Several Misconceptions, *Applied Catalysis B: Environmental*, **99:** 461–468 (2010).

[41] Arvis P., Guivarc'h-Levêque A., Varlan E., Colella C., Lehert P., Les Modèles Prédictifs de Grossesse en AMP Predictive Models for ART, *Journal de Gynécologie Obstétrique et Biologie de la Reproduction*, **42:** 12–20 (2013).

[42] Box G.E.P., Draper N.R., "Response Surfaces, Mixtures, and Ridge Analyses", 2nd ed, John Wiley & Sons, Inc, Hoboken, (2007).

[43] Nair A.T., Makwana A.R., Ahammed M.M., The Use of Response Surface Methodology for Modelling and Analysis of Water and Wastewater Treatment Processes: a Review, *Water Science and Technology*, **69:** 464–478 (2014).

[44] Boudechiche N., Mokaddem H., Sadaoui Z., Trari M., Biosorption of Cationic Dye from Aqueous Solutions onto Lignocellulosic Biomass (Luffa Cylindrica): Characterization, Equilibrium, Kinetic and Thermodynamic Studies, *Int. J. Ind. Chem.*, **7:** 167–180 (2016).

[45] Olivero R.A., Nocerino J.M., Deming S.N., Experimental Design and Optimization, *Chem. and Intelligent Laboratory Systems*, **42(1-2):** 3-40 (1998).

[46] Garcia B.B., Lourinho G., Romano P., Brito P.S.D., Photocatalytic Degradation of Swine Wastewater on Aqueous TiO_2 Suspensions: Optimization and Modeling via Box-Behnken Design, *Heliyon*, **6:** e03293 (2020).

[47] Sebti A., Boutra B., Trari M., Igoud S., Solar Photodegradation of Solophenyl Red 3BL and Neuro-Fuzzy Modeling: Kinetic, Mechanism and Mineralization Studies, *Reac. Kinet. Mech. Cat.*, **135:** 2207-2229 (2022).

[48] Arslan-Alaton I., Tureli G., Olmez-Hanci T., Treatment of Azo Dye Production Wastewaters Using Photo-Fenton-Like Advanced Oxidation Processes: Optimization by Response Surface Methodology, *Journal of Photochemistry and Photobiology A: Chemistry*, **202:** 142–153 (2009).

[49] Abdel-Maksoud Y., Imam E., Ramadan A., TiO_2 Solar Photocatalytic Reactor Systems: Selection of Reactor Design for Scale-Up and Commercialization—Analytical Review, *Catalysts*, **6:** 138 (2016).

[50] Bandala E.R., Estrada C., Comparison of Solar Collection Geometries for Application to Photocatalytic Degradation of Organic Contaminants, *Journal of Solar Energy Engineering*, **129:** 22–26 (2007).

[51] Spasiano D., Marotta R., Malato S., Fernandez-Ibañez P., Di Somma I., Solar Photocatalysis: Materials, Reactors, Some Commercial, and Pre-Industrialized Applications. A Comprehensive Approach, *Applied Catalysis B: Environmental*, **170–171:** 90–123 (2015).

[52] Bolton J.R., Bircher K.G., Tumas W., Tolman C.A., Figures-of-Merit for the Technical Development and Application of Advanced Oxidation Technologies for Both Electric- and Solar-Driven Systems (IUPAC Technical Report), *Pure and Applied Chemistry*, **73:** 627–637 (2001).

[53] Collivignarelli M.C., Carnevale Miino M., Arab H., Bestetti M., Franz S., Efficiency and Energy Demand in Polishing Treatment of Wastewater Treatment Plants Effluents: Photoelectrocatalysis vs. Photocatalysis and Photolysis, *Water*, **13:** 821 (2021).

[54] Rao N.N., Chaturvedi V., Li Puma G., Novel Pebble Bed Photocatalytic Reactor for Solar Treatment of Textile Wastewater, *Chemical Engineering Journal*, 184 90–97 (2012).

[55] Zaruma-Arias P.E., Núñez-Núñez C.M., González-Burciaga L.A., Proal-Nájera J.B., Solar Heterogenous Photocatalytic Degradation of Methylthionine Chloride on a Flat Plate Reactor: Effect of pH and H_2O_2 Addition, *Catalysts*, **12:** 132 (2022).